AIAA 91-2407

Computational Modeling of the Pressurization Process in a NASP Vehicle Propellant Tank Experimental Simulation

G.P. Sasmal, J.I. Hochstein, M.C. Wendl
Washington University,
St. Louis, Missouri

and

T.L. Hardy
NASA Lewis Research Center
Cleveland, Ohio

AIAA/SAE/ASME/ASEE
27th Joint Propulsion Conference
June 24-26, 1991 / Sacramento, CA

COMPUTATIONAL MODELING OF THE PRESSURIZATION PROCESS IN A NASP VEHICLE PROPELLANT TANK EXPERIMENTAL SIMULATION

G. P. Sasmal*, J. I. Hochstein**, M. C. Wendl*
Washington University, St. Louis, Missouri 63130

T. L. Hardy+
NASA Lewis Research Center, Cleveland, Ohio 44135

ABSTRACT

A multidimensional computational model of the pressurization process in a slush hydrogen propellant storage tank was developed and its accuracy evaluated by comparison to experimental data measured for a 5 ft diameter spherical tank. The fluid mechanic, thermodynamic, and heat transfer processes within the ullage are represented by a finite-volume model. The heat and mass fluxes at the ullage boundary were computed in auxiliary analyses and specified as input to the finite-volume model. The model was shown to be in reasonable agreement with the experiment data. A parameter study was undertaken to examine the dependence of the pressurization process on initial ullage temperature distribution and pressurant mass flow rate. It is shown that for a given heat flux rate at the ullage boundary, the pressurization process is nearly independent of initial temperature distribution. The mass flow rate study revealed decreasing pressurant mass requirement with increasing pressurant mass flow rate. Further, significant differences were identified between the ullage temperature and velocity fields predicted for pressurization of slush and those predicted for pressurization of liquid hydrogen A simplified model of the pressurization process was constructed in search of a dimensionless characterization of the pressurization process. It is shown that the relationship derived from this simplified model collapses all of the pressure history data generated during this study into a single curve.

Nomenclature

c_v	Specific heat at constant volume
h_g	Specific enthalpy of pressurant gas
$\dot{m}_g$	Pressurant mass flow rate
p	Tank pressure
$Q_{l/s}$	Heat transfer rate to liquid/slush H_2
Q_w	Rate of heat transfer to the tank wall
R	Gas constant
t	Time
t_p	Total pressurization time
T	Temperature
$\forall$	Tank ullage volume
ρ	Density of the gas in the tank

Subscripts

f	Final state
i	Initial state

INTRODUCTION

Vehicles which use cryogenic propellants because of their high specific impulse, incur the difficulties associated with managing the propellant prior to its use. The propellant management issue of interest in this study is the pressurization of a vehicle propellant storage tank prior to engine ignition. This pressurization may be required to alleviate feed-line cavitation problems or may provide the sole motive force for transporting propellant from the storage tank to the

* Research Associate, Member AIAA
** Associate Professor, Associate Fellow AIAA
\+ Aerospace Engineer, Member AIAA

engine. Since all methods proposed for tank pressurization require on-board resources (such as pressurant gas), optimization of the pressurization process is important for efficient vehicle design and operation. Optimization requires an understanding of the complex fluid dynamic and thermodynamic processes occurring in cryogenic propellant management systems and research into these processes has been pursued for over 20 years[1,2,3].

The proposal to use a mixture of solid and liquid hydrogen (known as slush hydrogen) as the storage medium for the National Aerospace Plane (NASP) presents a formidable challenge to understanding the pressurization process in the propellant storage tanks for such a vehicle. Modeling the pressurization process requires simultaneous solution of fluid mechanic, thermodynamic, and heat transfer models for a tank in which three phases of matter are present. Most existing models[1,4] are fundamentally one-dimensional and based on simplifying assumptions and experimentally derived correlations. Although these models have served well in the past, their range of validity is limited by the range of cases from which they are derived. It is not clear that they are adequate as design tools for future vehicle development. Since the flow field and temperature field in a tank during pressurization are in actuality multi-dimensional, it is reasonable to expect that accurate modeling of the pressurization process will require inclusion of the multi-dimensional effects. One study[5], using the same computational technology as the present study, has been performed to examine certain multidimensional effects. The current study was undertaken to identify or develop a tool for multidimensional modeling of the pressurization process and to use that tool to begin a study of the parametric dependence of the pressurization process.

The first phase of this study identified the FLOW-3D code[6] as a good candidate for modeling the pressurization process and demonstrated its accuracy by comparing computational predictions to experimental data. The second phase was a study of the parametric dependence of the pressurization process on initial ullage temperature distribution and pressurant mass flow rate . The third phase was development of a dimensionless characterization of pressurization by construction of a simplified model and examination of the physical processes which occur in the ullage during pressurization. The sections of this paper are organized to reflect this sequence of efforts. The final section summarizes the results of the entire study and presents conclusions drawn from these results.

Experiment Configuration

The experiment configuration modeled during this study was a 5 ft diameter spherical tank partially filled with liquid/slush hydrogen. The tank was pressurized by injecting gaseous hydrogen through a 1 ft diameter hemispherical diffuser located at the top of the tank. The pressurization process was initiated at the appropriate saturation pressure, (1.1 psia for slush hydrogen or 17.4 psia for liquid hydrogen), and was terminated when the tank internal pressure reached 50 psi. Although the experimental procedure then proceeded to a hold period followed by expulsion of the propellant, the focus of this study is on the pressurization process. A schematic of the tank configuration is shown in Fig. 1. A typical tank pressure history recorded during the pressurization of liquid hydrogen is shown in Fig. 2.

Evaluation of The Computational Model

The first phase of the study required identification or development of a computational tool capable of modeling the pressurization process. At a minimum, this requires the ability to model the transient low-speed compressible flow of an ideal gas, including heat transfer effects, in a reasonable representation of the geometry of interest. An important secondary consideration was the ability of the tool to also model the expulsion process. Since the fluid level in the tank changes during the expulsion process, this requires modeling the flow of an incompressible fluid with a vapor/liquid interface that changes position with time. The FLOW-3D

code[6] was selected as the highest rated candidate because it appeared to meet all of the basic requirements and because of previous successful applications to similar problems[5,8].

FLOW-3D is designed to model transient flows of fluid and thermal energy in three space dimensions in complicated geometries which may include free surfaces. Either Cartesian or cylindrical coordinates may be used to define the problem geometry and two-fluid calculations can be performed. Some of the models and features which contributed to selecting FLOW-3D for this study include: a compressible flow model (ideal gas), a two-fluid interface model, time-dependent boundary conditions, a thermal buoyancy model, a surface tension model, and a turbulent flow model. To efficiently use the available computational resources, the code is divided into a pre-processor, a main-processor, and a post-processor. The pre-processor resides on a VAX and is the interface through which the problem was defined. The data is then transferred to a Cray XMP where the main processor performs the analysis and generates the output files which are returned to the VAX for post-processing. A typical run for this study, using a two-dimensional pie-sector model of the tank, required approximately 25 minutes of CPU time on the Cray.

The first step in the evaluation process was to determine a suitable computational model for the spherical tank. Experimental data[1] obtained for pressurization of a tank with 56% ullage by volume was selected to test the performance of FLOW-3D. The free surface of the liquid hydrogen was modeled as a solid boundary to eliminate the need for a two-fluid model. Evaporation/condensation at the liquid free surface was neglected. Since detailed measurements of the pressurant gas flow rate were not obtained during preliminary analyses that the flow rate was a constant value computed by dividing the total mass added during the run by the pressurization time. Heat transfer rates to the tank wall and to the liquid/slush were taken from SLURP code analyses[4], (Q_w=5.02 Btu/sec,$Q_{l/s}$=0.46 Btu/sec). The diffuser at the pressurant gas inlet was modeled as a porous media.

Since all of the planned analyses were defined by axisymmetric boundary conditions for axisymmetric geometries, the first goal was to establish the validity of replacing a true three-dimensional model, (radial, azimuthal, axial), with a pie-sector model, (radial,1,axial), to reduce the computational demands for completing the study. The first configuration under examination was analyzed using a pie-sector model (10x1x10) and a fully three-dimensional model (10x36x10). Comparing the predicted velocity and temperature fields at a slice through a diameter of the fully three-dimensional model to those predicted by the pie-sector model revealed nearly identical solutions. To establish confidence that the pie-sector mesh was sufficiently refined, a convergence study was performed using a 15x1x15 mesh and a 10x1x20 mesh. Although the finer meshes revealed some details missing from the first mesh, the predicted fields for the finer meshes did not qualitatively differ from those predicted by the first mesh. Since the liquid free surface was modeled as a solid boundary with a specified heat flux, the improved temperature gradient near the free-surface predicted using the finer meshes is not a significant factor for these analyses, but could become significant for analyses in which heat and mass transfer at the free surface is computed. It was therefore concluded that a 10x1x10 pie-sector mesh would be used for all subsequent analyses in this study.

The second step in the evaluation process was to compare computational predictions to experimentally obtained data. Since the pressurant inlet pressure was not measured during the experiment, a value of 50 psi was assumed for the inlet pressure based on other known parameters in the experiment. The pressurant inlet mass flow rate is a key parameter which must be specified to the computational model but which was not recorded during the experiment. The S-curve of the pressure history displayed in Fig. 2 suggests that, contrary to initial assumptions, the flow rate during the experiment was a function of time. A sequence of

analyses were performed during which the flow rate history was iteratively adjusted until the pressure history predicted by FLOW-3D matched the history displayed in Fig 2.

The difference between measured and computationally predicted total mass added was less than 15%. Although this difference is larger than had been hoped for, several factors contributed to this difference. As detailed above, important input parameters, such as pressurant inlet pressure and flow rate history, were estimated or back-calculated because they had not been measured during the experimental effort. Given the level of uncertainty in the problem definition, the agreement between experimental and computational results was considered adequate to proceed with the investigation. To eliminate this uncertainty in future efforts, a list of recommended measurements for future experimental studies is provided in the concluding remarks of this paper.

Parametric Study of Pressurization Process

Table 1 presents a summary of the input parameters and the performance predictions for the twelve cases studied during this effort. An initial pressure of 17.4 psi indicates pressurization of liquid hydrogen whereas an initial pressure of 1.1 psia indicates that slush hydrogen was pressurized. For all analyses, the pressurant gas inlet pressure was specified to be 50 psi, the inlet temperature to be 307 °R, and the heat flux rates were specified to be Q_w=5.02 Btu/sec and $Q_{l/s}$=0.46 Btu/sec. The pressurant mass flow rate for each case was assigned a constant value which is listed in Table 1. The analysis matrix defined in Table 1 represents studies of different parametric effects which are described in detail in the balance of this section.

The first study focused on the influence of initial temperature distribution within the ullage on the pressurization process. The ullage temperature distribution had not been measured during the experimental investigation so two bounding cases

Table 1 Analysis Matrix (55.6% ullage)

Case #	*Initial Pressure (psia)	*Initial Temp. (°R)	*Inlet Velocity (ft/s)	**Press. Time (s)	**Mass Added (lb_m)	**Flow Rate (lb_m/s)	**Final Pressure (psia)
1	17.4	60-40	1.393	33.0	0.771	0.0234	50.2
2	1.1	60-40	1.393	54.0	1.262	0.0234	49.8
3	17.4	250-40	1.655	26.0	0.720	0.0277	49.8
4	17.4	60-40	1.655	26.0	0.720	0.0277	49.8
5	1.1	60-40	1.655	43.0	1.193	0.0277	50.4
6	1.1	250-40	1.655	43.0	1.193	0.0277	50.4
7	17.4	60-40	2.500	15.5	0.649	0.0419	49.5
8	1.1	60-40	2.500	25.5	1.070	0.0419	50.1
9	17.4	60-40	3.500	10.5	0.612	0.0583	49.3
10	1.1	60-40	3.500	17.0	0.992	0.0583	49.2
11	17.4	60-40	5.000	7.2	0.600	0.0832	49.7
12	1.1	60-40	5.000	11.5	0.958	0.0832	49.3

* specified value
** computationally predicted value

were selected: the 60-40 °R distribution was selected to represent a fairly well mixed ullage whereas the 250-40 °R distribution was selected to represent a thermally stratified ullage. The temperature fields predicted at the end of the pressurization process for both temperature distributions and for both propellants (cases 3, 4, 5, 6) are displayed in Fig. 3. Review of Table 1 reveals that, given the same heat flux rate at the tank wall, the pressurization time appears to be independent of initial ullage temperature distribution. Although the global pressurization performance as measured by total mass added and pressurization time is unchanged by the different initial ullage temperature distributions, the detailed temperature profiles do show some differences. In particular, the clustering of temperature contours at the surface of the slush hydrogen (for the low intial pressure) indicates that there may be a significant difference in heat transfer and mass transfer rates at the slush/vapor interface than at the liquid/ vapor interface. Since the current model uses a specified heat transfer rate at the free surface, and assumes zero mass transfer at the free surface, this hypothesis is unprovable with the present modeling capability and remains a topic for future study.

The relationship between pressurization time and pressurant flow rate revealed by the matrix of cases in Table 1 is displayed in Fig. 4. Although the decrease in pressurization time with increasing mass flow rate is expected, it should be noted that the relationship is not a simple inverse proportionality. Figures 5 and 6 present one of the most interesting results of the study. The computationally predicted relationship between pressurization time and the total pressurant mass addition required to pressurize the tank to 50 psi is displayed in Fig. 5. The relationship between pressurant mass flow rate and the total mass addition required is displayed in Figure 6. The two relationships are consistent and lead to the conclusion that a more rapid pressurization requires less pressurant mass than a slow pressurization. Although this conclusion may be counterintuitive, the explanation lies in the imposed thermal boundary conditions. A longer pressurization time, coupled with the constant heat flux specified at the tank walls and at the liquid/slush interface, results in a greater cooling of the ullage. At the lower vapor temperature, a greater vapor mass is required to reach the desired pressure level. Review of the SLURP study report[4] reveals data to support this conclusion and a comment on this trend by those researchers. Therefore, the ability of the FLOW-3D model to correctly predict this trend lends additional confidence to the validity of the computational model, and brings additional attention to this interesting and potentially important phenomena.

The dependence of velocity and temperature fields in the ullage at the end of pressurization on the pressurant mass flow rate was examined by extracting appropriate data from the results generated by the analysis matrix defined in Table 1. All the analyses examined for this study began with the 60-40 °R ullage temperature distribution and proceeded from an initial saturation pressure to a final pressure of 50 psi. Figure 7 presents computed velocity fields in the ullage for pressurization of liquid hydrogen and Fig. 8 presents the corresponding temperature fields. For the range of inlet mass flow rates examined, the entering gas jet never fully penetrated into the ullage volume. As the flow rate increases a vortex is established at the top of the tank near the inlet diffuser. The temperature near the free surface varies from 50.5 °R to 57.4 °R for the range of pressurant mass flow rates studied. Although the presence of the jet is apparent in the temperature contours, the bulk of the ullage space is well represented by an axial temperature distribution with little radial dependence.

The velocity fields computed for pressurization of slush hydrogen are presented in Fig. 9 and the corresponding temperature fields in Fig. 10. Comparing Fig. 9 to Fig. 7 reveals that substantially different flow patterns are established during slush pressurization than during liquid pressurization. At the lower flow rates, the incoming jet again fails to fully penetrate the ullage and establishes a vortical flow near the inlet. At the higher flow rates, the incoming pressurant jet is seen to fully penetrate the ullage

volume and to establish a variety of flow patterns. At an intermediate flow rate, the jet penetrates all the way to the slush surface and then follows a serpentine path establishing two side-by-side vortices. At the highest flow rate, the jet penetrates to the slush surface and moves radially outward along the surface toward the tank wall. Although two vortices are again formed, they are arranged one-above-the-other instead of side-by-side. Examining Fig. 10 shows that the variety of flow patterns predicted for slush pressurization is reflected in the variety of ullage temperature distributions. At the higher flow rates, the uniformity of temperature with radial location observed for liquid pressurization is replaced with highly radially dependent temperature distributions. The predicted ullage temperature near the slush surface increases from 169 °R for the lowest inlet mass flow rate to 286 °R for the highest flow rate, as compared to approximately 60 °R for the liquid cases.

Comparing the predicted temperature and velocity fields for pressurization of liquid hydrogen to those predicted for slush hydrogen revealed some significant differences. These differences in turn raise concern about some of the modeling assumptions used to perform the analyses. The highly stratified ullage temperature distributions produced by pressurization of liquid hydrogen lead to relatively low gas temperatures near the liquid/vapor interface which, when coupled with the nearly stagnant state of gas near the free surface, seem to support the modeling assumption of constant heat flux with negligible mass transport at the liquid/vapor interface. In contrast, high gas temperatures predicted during pressurization of the slush, coupled with significant flow velocities predicted near the free surface, lead one to seriously question this modeling assumption. Since evaporation or condensation can have a significant effect on the tank internal pressure, caution should be used in accepting computational predictions which do not include these effects. To definitively resolve this concern requires modeling capabilities beyond the those of the present computational tool.

The evolution of temperature and velocity fields observed during the inlet mass flow rate dependence study naturally lead to a curiosity about the dependence of the tank pressure history on inlet mass flow rate. Figure 11 displays the tank pressure histories predicted for pressurization of liquid hydrogen. The tank pressure histories predicted for pressurization of slush are displayed in Fig. 12. Although the trends are not surprising, it should be noted that the rate-of-change of pressure is not constant during the pressurization process but rather increases slightly with increasing elapsed time. A desire to understand this behavior lead to the modeling and dimensional analysis described in the next section.

A Simplified Model and Non-Dimensional Characterization

If multidimensional effects of the pressurization process are neglected, and the ullage is modeled as a lumped thermodynamic entity, a simplified analytical model of the pressurization process can be readily developed. Conservation of thermal energy can be enforced by satisfying a balance equation written for the ullage volume:

$$c_v \forall \frac{d(\rho T)}{dt} = \dot{m}_g h_g - Q_w - Q_{l/s} \qquad [1]$$

where Q_w includes any discrete "heat leaks" into the ullage as well as convective heat transfer from the ullage to the tank wall. The product of density with temperature in the derivative can be replaced by an expression including pressure by assuming that the ullage can be modeled as an ideal gas ($\rho T = p/R$).

$$\frac{dp}{dt} = \frac{R}{c_v \forall} (\dot{m}_g h_g - Q_w - Q_{l/s}) \qquad [2]$$

This form clearly shows that, for constant specified heat flux at the boundaries and constant pressurant mass flow rate, this lumped model predicts a constant rate-of change of tank internal pressure with time. This is in qualitative agreement with the near-constant pressurization rate predicted

by the computational model. The difference is due to the multidimensional effects incorporated into the computational model which cannot be included in the simple lumped model.

Since one goal of the modeling and analysis is to develop correlating parameters for the pressurization process, it is important to select appropriate normalizing or non-dimensionalizing scales. One logical time scale is the elapsed time required to complete the pressurization process.

$$t^* = \frac{t}{t_f} \qquad [3]$$

The total change in pressure to be accomplished by the pressurization process was selected to normalize the pressure rise from pressurization initiation.

$$p^* = \frac{p - p_i}{p_f - p_i} \qquad [4]$$

It was hoped that this combination of characteristic scales would produce a nondimensional representation of the pressurization process which would produce a single relationship for all the pressurization cases. Combining the nondimensional variables defined in Eqs. 3 and 4 produces the following expression for the rate-of-change of nondimensional pressure with normalized time.

$$\frac{dp^*}{dt^*} = \frac{d\left(\frac{p - p_i}{p_f - p_i}\right)}{d\left(\frac{t}{t_f}\right)} = \left(\frac{t_f}{p_f - p_i}\right)\frac{dp}{dt} \qquad [5]$$

Recalling that dp/dt is constant for constant heat flux and flow rate boundary conditions, integrating this expression over the elapsed time required for pressurization yields the following result.

$$p_f^* - p_i^* = \left(\frac{t_f}{p_f - p_i}\frac{dp}{dt}\right)(t_f^* - t_i^*) \qquad [6]$$

Rearranging, and substituting appropriate values into this equation, produces the following result.

$$\left(\frac{t_f}{p_f - p_i}\right)\frac{dp}{dt} = \frac{p_f^* - p_i^*}{t_f^* - t_i^*} = \frac{1 - 0}{1 - 0} = 1 \qquad [7]$$

Therefore, for any pressurization analysis with specified constant mass inflow rate and constant heat flux boundary conditions:

$$\frac{dp^*}{dt^*} = 1 \ . \qquad [8]$$

Since this result is independent of specific values for any of the parameters required for the computation, the goal of a "universal" relationship for all pressurization processes has been satisfied (for the lumped parameter model).

Since the computational model includes multidimensional effects which cannot be included in the lumped parameter model, the validity of dp^*/dt^* as a correlating parameter for pressurization analyses must be evaluated against the results from the analysis matrix defined in Table 1. The tank pressure history data previously displayed in Figs. 11 and 12 were reorganized using the new dimensionless variables to produce Fig. 13. Careful examination reveals that, although dp^*/dt^* is not precisely equal to a constant value of one, reorganizing the data using p^* and t^* does collapse all the data into a single curve. The deviation of this curve from a straight line is similar to that seen in the dimensional plots and is due to multidimensional effects.

Summary and Concluding Remarks

The proposal to use slush hydrogen as the propellant storage medium for the NASP presents a formidable challenge to the design and efficient operation of the propellant management system. Previous studies of propellant tank pressurization prior to main engine ignition have primarily involved experimental measurements in model tanks[1,2] or analytical and computational models based on lumped or one-dimensional

models[4]. The present study was initiated: to develop a capability for multidimensional modeling of the propellant tank pressurization process prior to main engine ignition; to evaluate the performance of, and identify limitations in, the model and; to begin evaluation of the parametric dependence of the pressurization process on the system initial conditions and boundary conditions.

After a review of available computational tools, the FLOW-3D code was selected as the most promising candidate for modeling pressurization and expulsion of slush hydrogen from storage tanks. Code performance was evaluated by comparing computational predictions to measurements obtained during the pressurization of an experimental simulation of a NASP propellant tank[1]. The analyses demonstrated that, despite significant uncertainties in problem definition due to incomplete specification of the experiment conditions, a pie-sector (axisymmetric) computational model was able to replicate the tank pressure history and to predict the total pressurant mass required for the pressurization to within 15% of the measured value. Based on this evaluation, it was concluded that FLOW-3D is a suitable tool from multidimensional modeling of the pressurization process.

Typical of many efforts to verify computational tools by comparison to experiment data not specifically obtained for this purpose, the performance evaluation was complicated by the absence from the experiment report of key parameters required to define the model. To help eliminate uncertainties in model definition, future experiments should include measurement of: the history of pressurant inlet pressure, temperature, and mass flow rate; the initial temperature distribution within the ullage; the history of heat loss to the tank wall and to the slush/vapor interface and; the rate of evaporation or condensation at the free surface. Measurements necessary to evaluate code performance should include the pressure history in the tank and the transient velocity and temperature fields in the ullage during pressurization. Although it is recognized that the distinction between model definition and performance evaluation measurements is tenuous, and that some of the requested measurements are difficult to obtain, the lists have been assembled as a starting point for consideration by future efforts.

The dependence of the pressurization process on initial ullage temperature distribution was examined by comparing predictions for a 60-40 °R distribution, representing a well mixed initial condition, to those for a 250-40 °R distribution, representing a thermally stratified initial condition. For the pressurant mass flow rates considered and the heat flux rate specified at the ullage boundary, the global performance as measured by elapsed time required for the pressurization and the total pressurant mass added appears to be nearly independent of the initial ullage temperature distribution. Review of the predicted velocity and temperature fields near the free surface at the end of pressurization indicates that the assumption of no mass transfer at this interface merits future scrutiny. Further, the specification of a single heat flux rate at the tank wall for all cases is also suspect and should be replaced by a more accurate model when possible.

A study of the effect of pressurant mass flow rate on the pressurization process revealed an interesting trend as well as potentially significant differences between pressurization of liquid hydrogen and pressurization of slush hydrogen. For both liquid and slush cases, the pressurant mass required to reach the desired pressure level decreases with increasing pressurant mass flow rate. This is in accord with experiment data[1] and is discussed in detail in the preceding section. Review of the temperature and velocity fields predicted for the slush and liquid cases during this study revealed interesting differences between the cases. At comparable pressurant mass flow rates, the inlet jet fully penetrates the ullage of the slush cases whereas it does not for the liquid cases. This difference leads to significantly different flow and temperature fields in the ullage. The temperature field predicted for the liquid cases has little radial dependence and the one-dimensional model provided by the SLURP code[4] is probably reasonable. In

contrast, the temperature fields predicted for pressurization of slush have a very significant radial dependency and will not be well represented by a one-dimensional model. Further, at the higher mass flow rates, the temperatures and velocities near the free surface of the slush are significantly higher for the slush cases than for the liquid cases. The low values predicted for the liquid cases suggest that the assumption of no mass transfer at the free surface may be reasonable whereas the high values for the slush case cast serious doubt on the validity of such an assumption.

A simplified model of the pressurization process was developed in search of a nondimensional characterization of the process. Based on this model, a dimensionless time was defined as elapsed time from pressurization initiation normalized by the time required to complete pressurization. A dimensionless pressure was defined by the increase in pressure from initial pressure divided by the total pressure rise to be accomplished. Using these dimensionless parameters, it was demonstrated that the tank pressure history for all of the cases in this study collapse into a single curve. Although the relationship revealed by this study lacks predictive capability since the dimensionless parameters contain variables which are not known a priori, it is valuable for unifying the presentation of data from experimental and computational studies of the pressurization process.

Acknowledgments

This research was made possible by the support of the NASA Lewis Research Center provided through NASA Grant NAG3-1156.

References

[1] Stochl, R.J., "Gaseous Hydrogen Requirements for the Discharge of Liquid Hydrogen from a 1.52 m (5ft) Diameter Spherical Tank", NASA TND-5336, August 1969.

[2] Stochl, R.J., "Gaseous Helium Requirements for the Discharge of Liquid Hydrogen from a 1.52 m (5ft) Diameter Spherical Tank", NASA TND-5621, January 1970.

[3]Aydelott, J.C., Carney, M.J., and Hochstein, J.I., "NASA Lewis Research Center Low-Gravity Fluid Management Technology Program," NASA TM-87145, November 1985.

[4]Hardy, T.L. and Thomsik, T.M., "SLURP: A Computer Code for Pressurization of a Slush Hydrogen Tank Using Gaseous Hydrogen or Helium," NASP TM-1088, January 1990.

[5]Hardy, T.L. and Tomsik, T.M., "Prediction of Ullage Gas Thermal Stratification in a NASP Vehicle Propellant Tank Experimental Simulation Using FLOW-3D," NASA TM-103217, July 1990.

[6]"FLOW3D: Computational Modeling Power for Scientists and Engineers," Flow Science Inc, Los Alamos, New Mexico, 1988.

[7]Navikas, J., Cady, E.C., Flaska, T.L., "Modeling of Solid-Liquid Circulation in National Aerospace Plane's Slush Hydrogen Tanks", 24th Joint Propulsion Conference, Boston, Massachusetts, 11-14 July 1988.

[8]Hochstein, J.I., "Computational Prediction of Propellant Motion During Separation of a Centaur G-Prime Vehicle From the Shuttle", Report No. WU/CFDL-85/1, Washington University, St. Louis, December 1985.

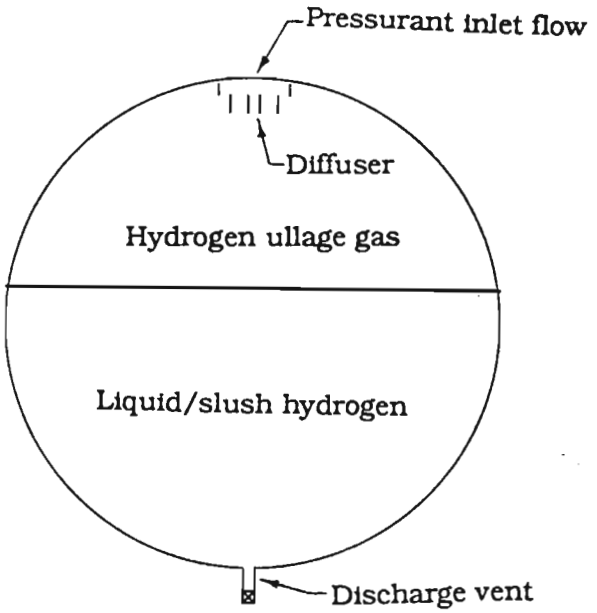

Figure 1 Schematic of experiment tank

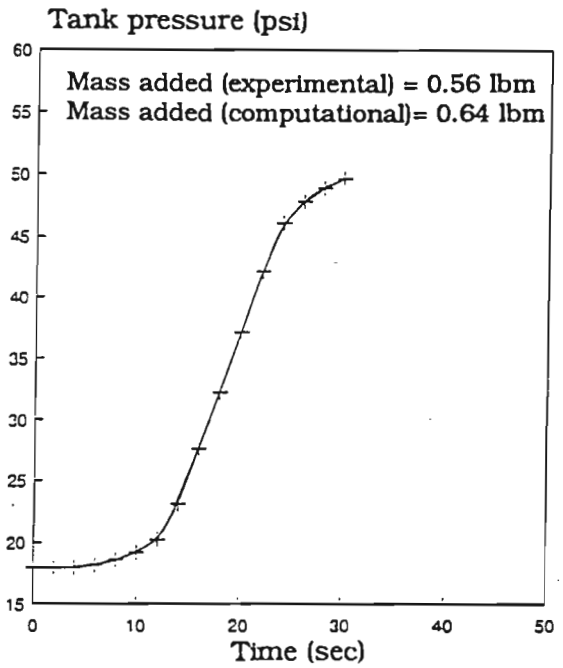

Figure 2 Pressurization of tank containing liquid hydrogen (55.6 % ullage)

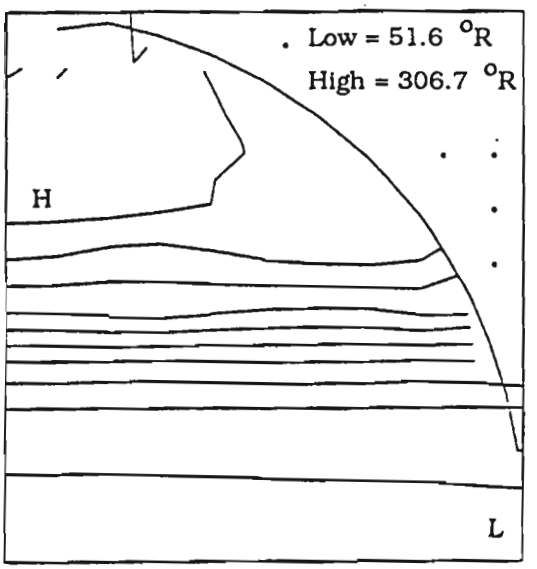

(a) Case # 4

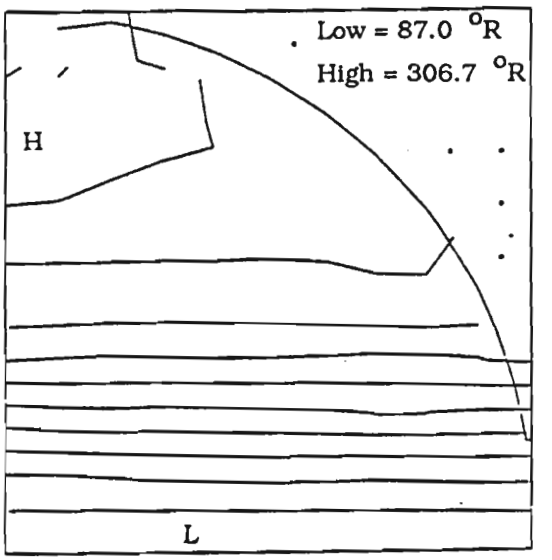

(b) Case # 3

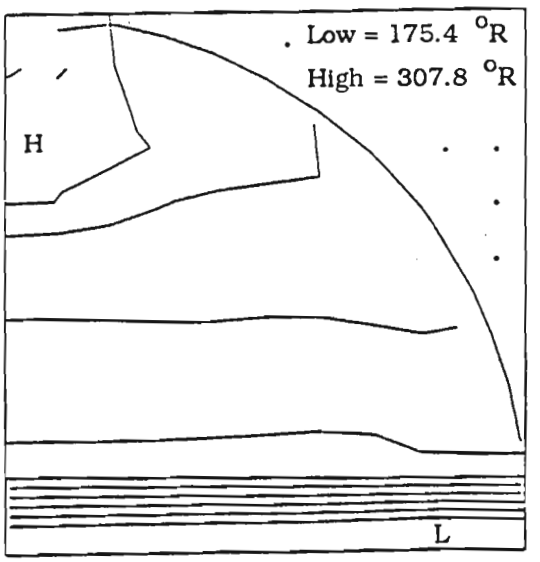

(c) Case # 5

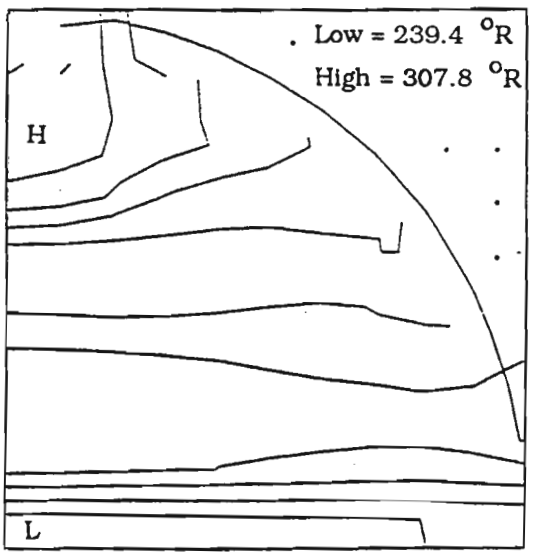

(d) Case # 6

Figure 3 Temperature distribution at the end of pressurization ($\dot{m}$ = 0.277 lbm/s)

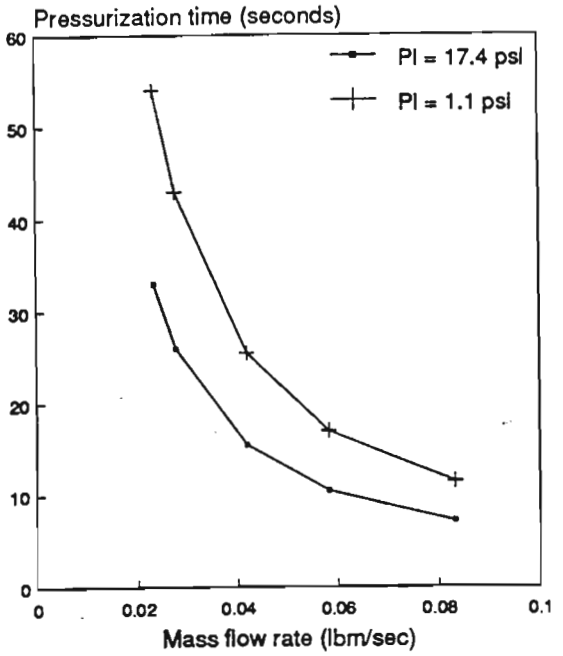

Figure 4 Pressurization time .vs. Mass flow rate

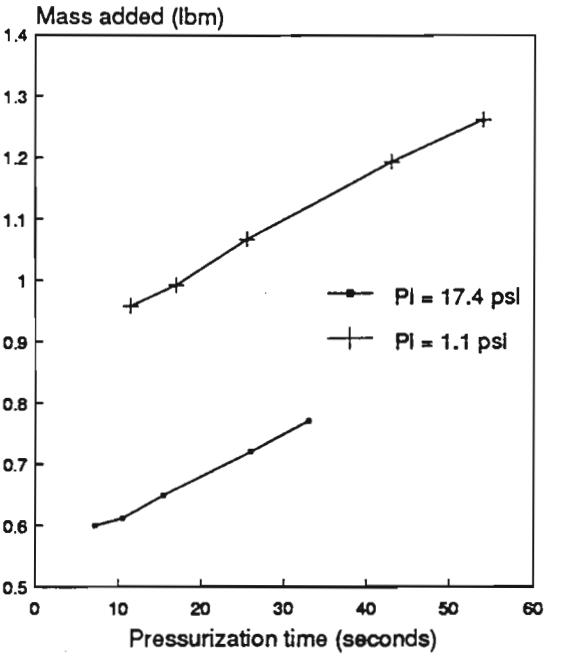

Figure 5 Mass added .vs. Pressurization time

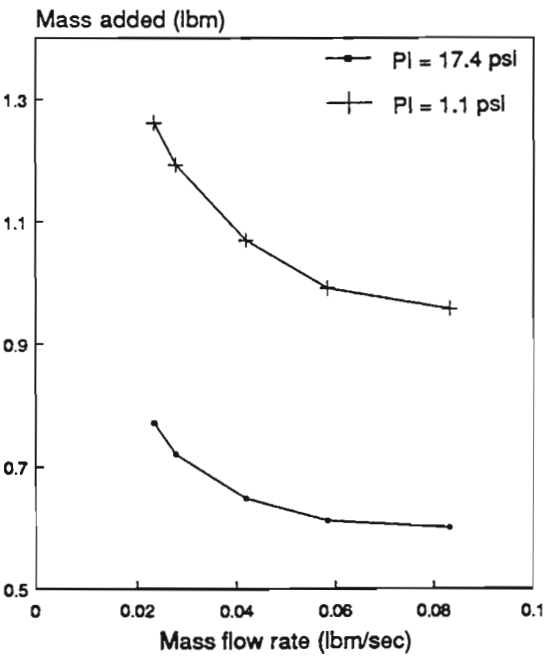

Figure 6 Mass added .vs. Mass flow rate

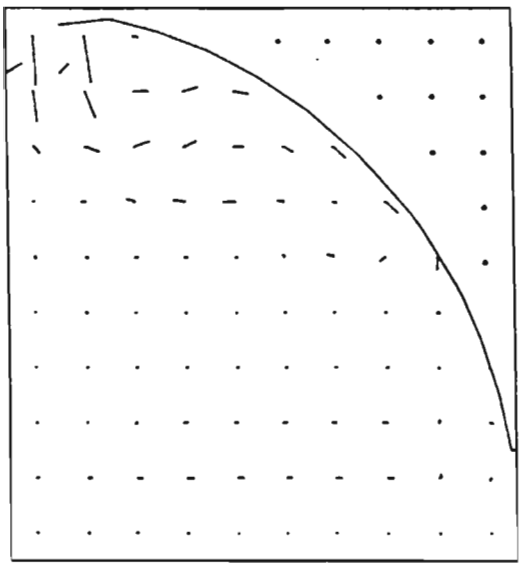

(a) Case # 1

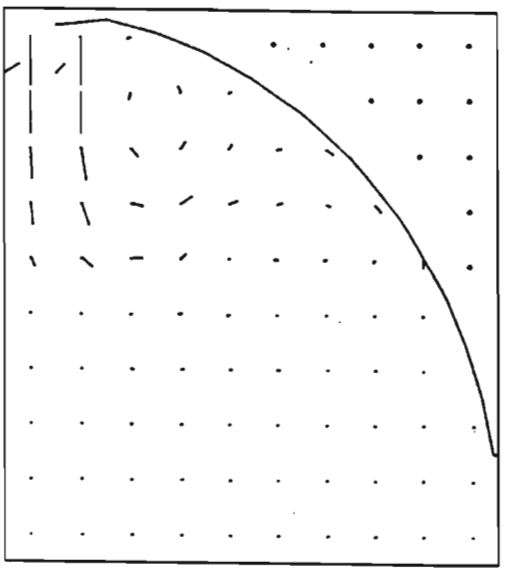

(b) Case # 7

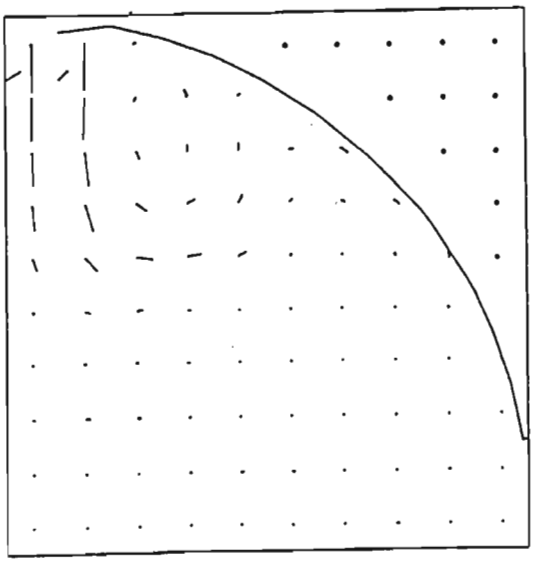

(c) Case # 9

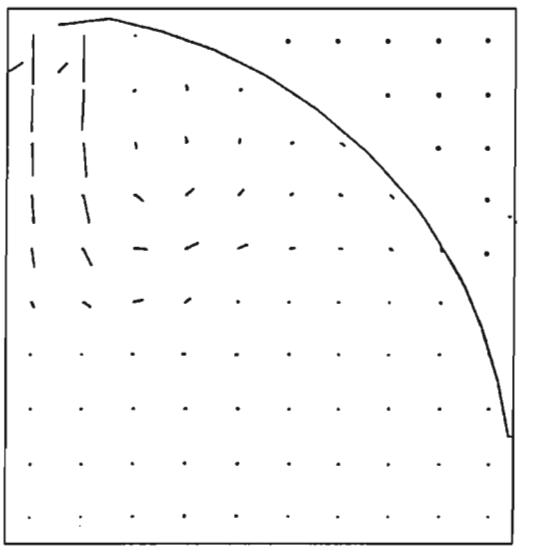

(d) Case # 11

Figure 7 Velocity fields for pressurizing liquid hydrogen

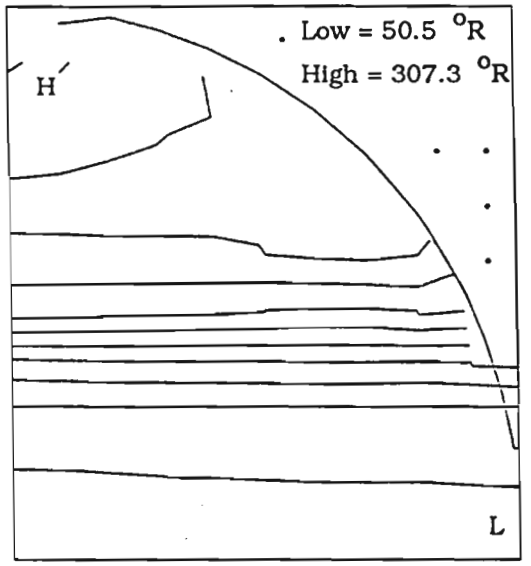

(a) Case # 1

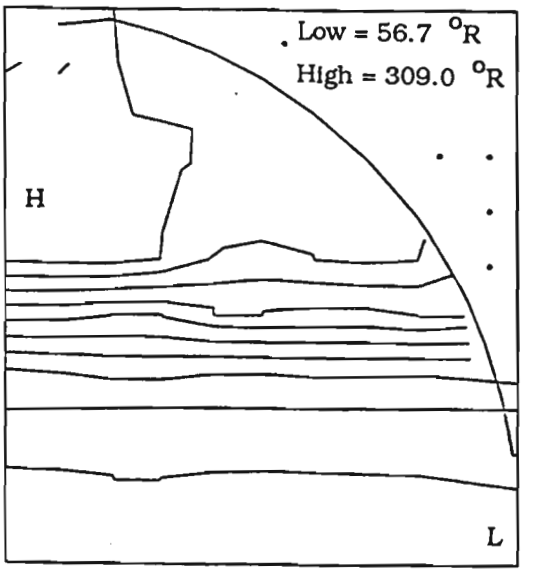

(b) Case # 7

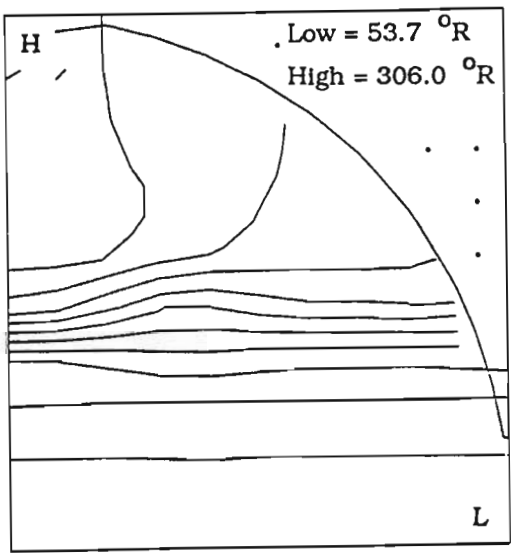

(c) Case # 9

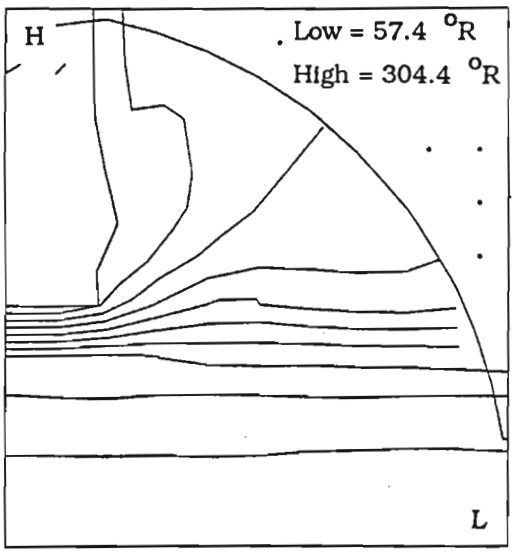

(d) Case # 11

Figure 8 Temperature fields for pressurizing liquid hydrogen

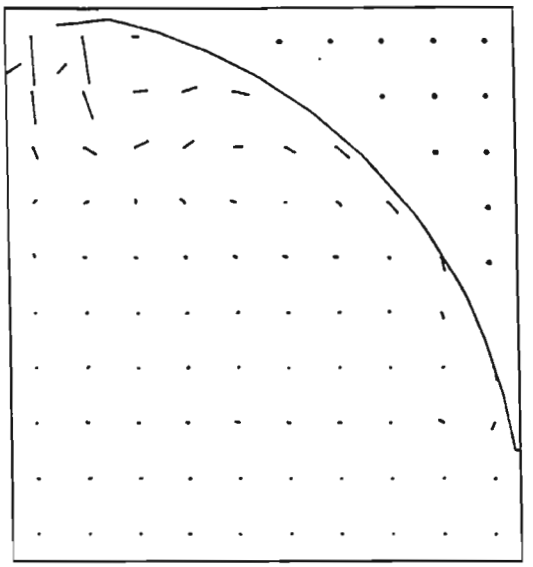

(a) Case # 2

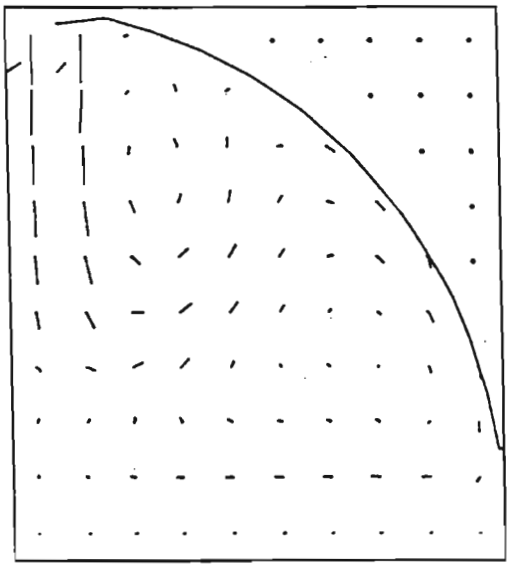

(b) Case # 8

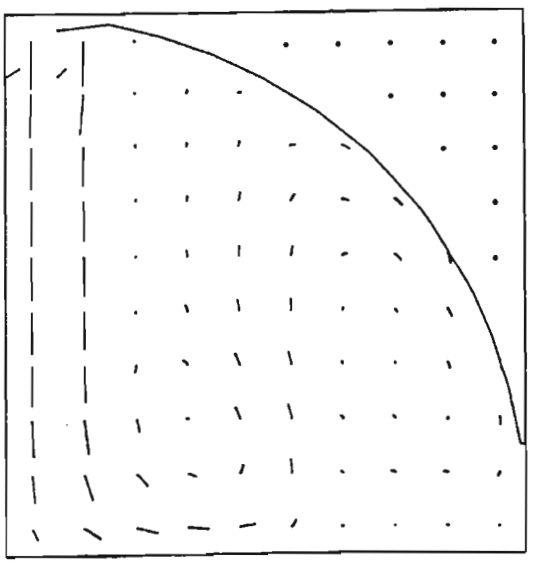

(c) Case # 10

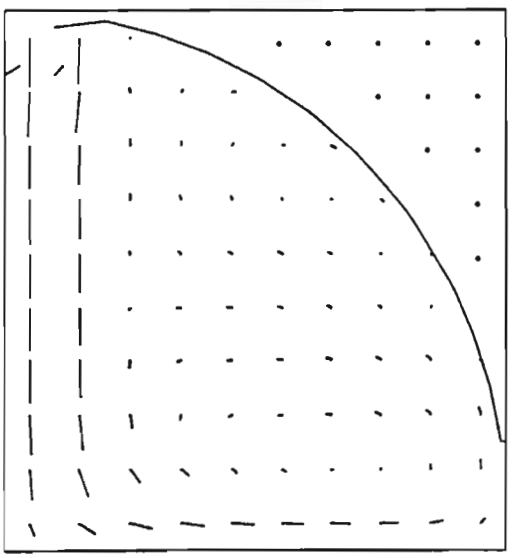

(d) Case # 12

Figure 9 Velocity fields for pressurizing slush hydrogen

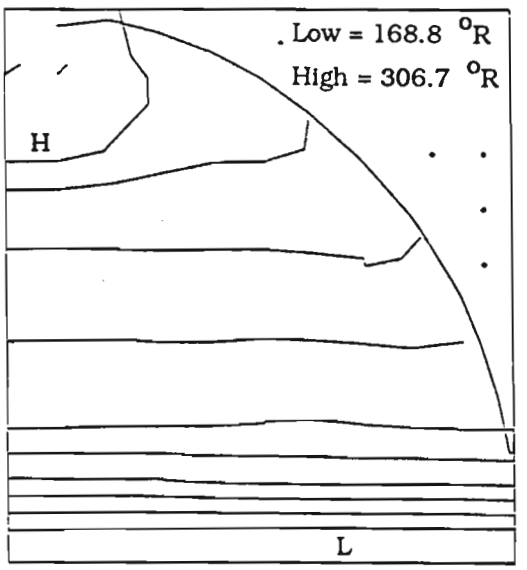

(a) Case # 2

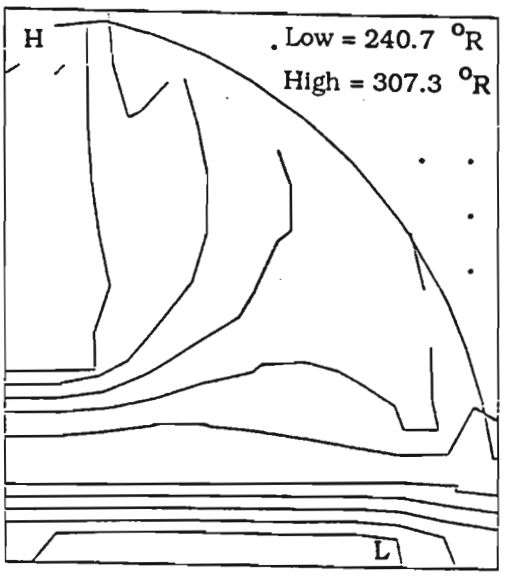

(b) Case # 8

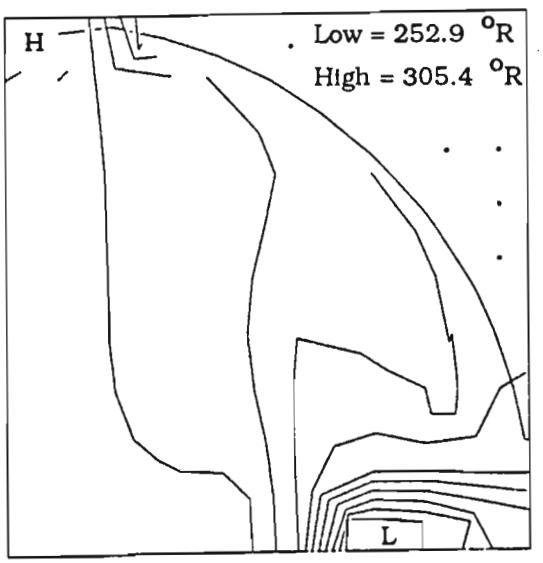

(c) Case # 10

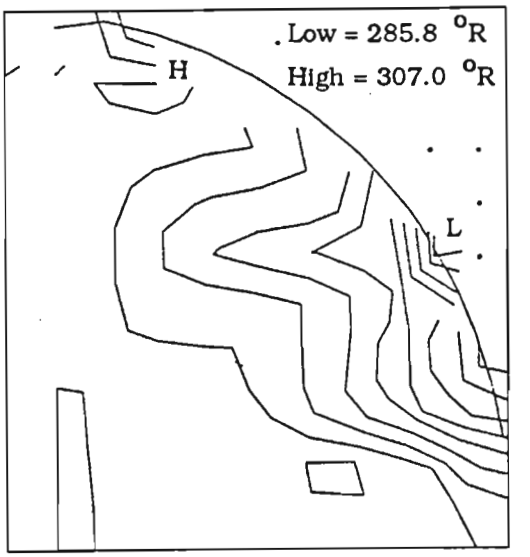

(d) Case # 12

Figure 10 Temperature fields for pressurizing liquid hydrogen

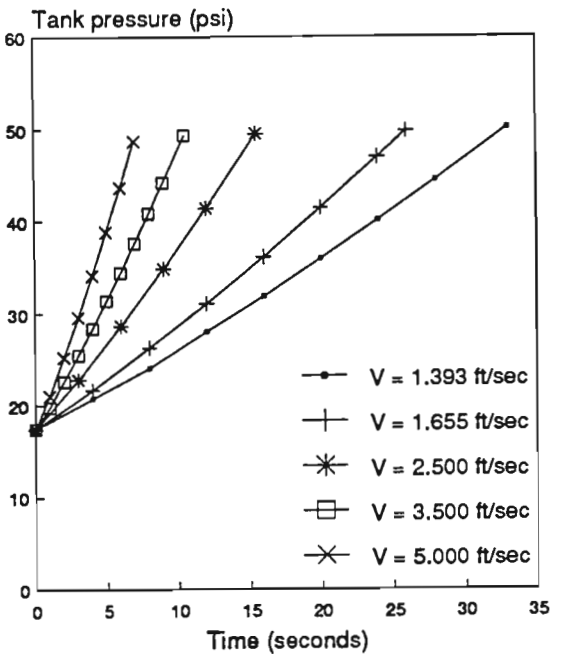

Figure 11 Tank pressure history (liquid hydrogen)

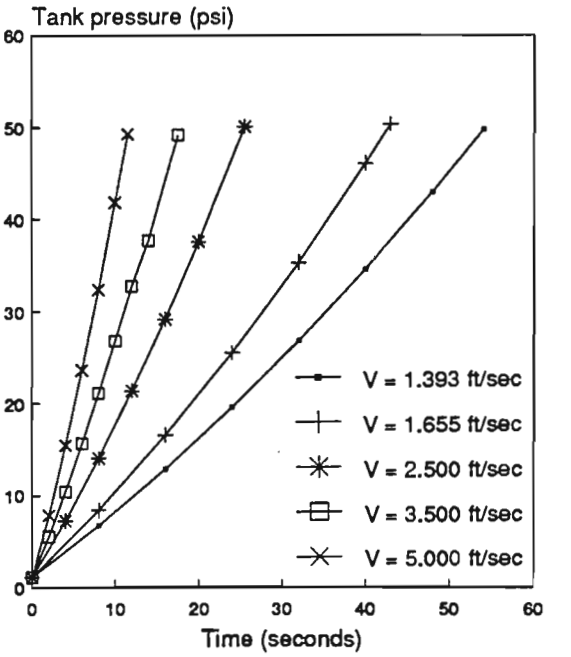

Figure 12 Tank pressure history (slush hydrogen)

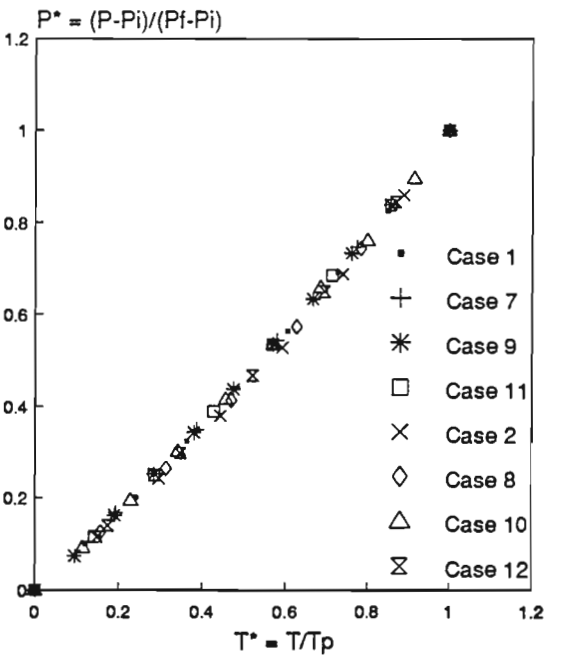

Figure 13 Dimensionless pressure .vs. normalized time